Far Infrared Spectra of $Al_2O_3:Cr^{3+}$ and $Al_2O_3:Ti^{3+}$†

E. D. NELSON, J. Y. WONG, AND A. L. SCHAWLOW
Stanford University, Stanford, California
(Received 10 October 1966)

The absorption spectrum of ruby containing 1% Cr_2O_3 has been observed at 77°K and below, over the range from 10 to 160 cm^{-1}, using a large grating spectrometer. Although chromium ion pairs are known to have energy-level intervals in this region, no absorption lines were observed, even in a sample 15-cm long. Thus, these spin-changing transitions are, as might be expected, quite forbidden. In $Al_2O_3:Ti^{3+}$, levels were observed at 37.8 and 107.5 cm^{-1} with strong transitions connecting them. A broad lattice absorption was also observed. The position of the 37.8-cm^{-1} level is in reasonable agreement with predictions from earlier microwave relaxation measurements in the ground state. The infrared linewidths are large, indicating a rapid relaxation without spin flip. The level spacings are smaller than predicted by crystal-field theory, indicating that the effective trigonal field and spin-orbit coupling are reduced by a dynamic Jahn-Teller effect.

I. INTRODUCTION

IT has been shown by Hadni *et al.*[1] and by Chang and Rowntree[1] that much of the far infrared lattice absorption of crystals can be reduced by cooling the crystals to low temperatures. The temperature-dependent part of the lattice absorption is due to the combination of an incoming photon with a thermally excited acoustic phonon to give an optical phonon. At low temperatures few acoustic phonons are available for this type of absorption.

In particular, Hadni has shown that the Al_2O_3 lattice is nearly transparent in the far infrared for temperatures less than 77°K.[2] Thus, it is possible to study the spectra of ions in the Al_2O_3 lattice. We present here the far infrared absorption spectra for $Al_2O_3:Cr^{3+}$ and for $Al_2O_3:Ti^{3+}$.

II. EXPERIMENTAL APPARATUS

In order to do far infrared spectroscopy of ions in crystals and also to do experiments on far infrared lasers, we have constructed a large grating spectrometer. At the present time we have gratings and filters to cover the spectral region from 8.3 to 162 cm^{-1}. A grating instrument was chosen over the higher-resolution Michelson interferometer[3] because the interferometer is not suited for work with high-power single-pulse lasers.

The spectrometer has $f/4$ Ebert optics; the Ebert mirror has a 40-in. focal length. A 7-ft long by $2\frac{1}{2}$-ft. diam cylindrical aluminum vacuum tank houses the entire spectrometer, including source and entrance optics. Thus, atmospheric water vapor [which absorbs infrared (i.r.) radiation] can be pumped out of the radiation path. The cylindrical tank is split in half horizontally so that the top can be raised easily by a pulley arrangement to provide access to the spectrometer components.

Figure 1 shows the experimental arrangement applicable to the experiments to be described here. Note that all spectroscopy is done in *absorption*. The spectrometer output is monochromatic far i.r. radiation (chopped at 10 cps), that is conveyed via a 1.1-cm i.d. aluminum light pipe to the absorbing sample mounted at the bottom of a large metal Dewar. The actual sample-mounting technique will be described separately for each experiment. A crystalline quartz window separates the high-vacuum Dewar compartment from the relatively low-vacuum spectrometer tank and allows gratings to be changed while the Dewar remains at low temperatures. After passing through the sample, the radiation is conveyed by light pipe to the Texas Instruments germanium bolometer detector which operates at 4.2°K. The detector output (an electrical signal) is amplified approximately 1000-fold by the preamplifier and then fed into the signal channel of the Princeton lock-in amplifier. The lock-in amplifier reference channel receives a reference signal (chopped

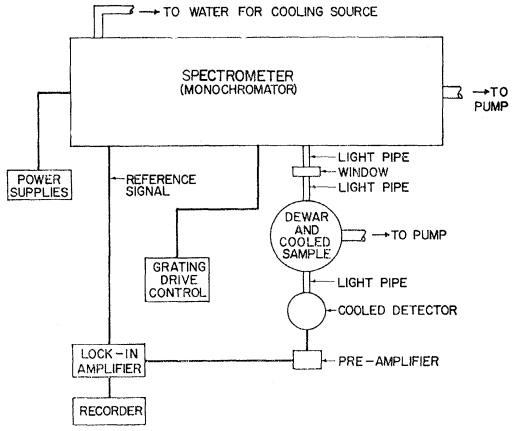

FIG. 1. Block diagram of the far infrared spectrometer and auxiliary equipment.

† Work supported by the National Aeronautics and Space Administration under Grant No. NsG 331.

[1] A. Hadni, B. Wyncke, P. Strimer, E. Decamps, and J. Claudel, in *Proceedings of the Third International Congress of Quantum Electronics*, edited by P. Grivet and N. Bloembergen (Columbia University Press, New York, 1964), p. 731; W. S. C. Chang and R. F. Rowntree, *ibid.*, p. 677.

[2] A. Hadni, Phys. Rev. **136**, A758 (1964).

[3] P. L. Richards, in Proceedings of the Far Infrared Physics Symposium, Riverside, California, 1964 (unpublished).

at 10 cps by the same chopper that chops the far i.r. signal) from the spectrometer so that the lock-in amplifier will amplify only those signals from the preamplifier that lie within a certain bandwidth (determined by a *RC* time constant) about the chopper frequency of 10 cps. The slowly varying dc output of the lock-in amplifier is recorded on chart paper.

III. $Al_2O_3:Cr^{3+}$

A. Introduction

The energy levels of a single Cr^{3+} ion in dilute ruby (0.05% or less of Cr_2O_3 in Al_2O_3) are known theoretically[4] and experimentally.[5] The $^4A_2$ ground state is split by only 0.38 cm^{-1}, while the next state, the ^2E, is 14 400 cm^{-1} above the ground state. Hence, there are no low-lying far i.r. levels for the single Cr^{3+} ion in Al_2O_3.

The optical spectrum of concentrated ruby ($\sim$0.1 to $\sim$1.0% Cr_2O_3 in Al_2O_3) contains numerous lines that increase in intensity nearly as the square of the chromium-ion concentration. These lines can be attributed to coupled pairs of Cr^{3+} ions.[6] Analysis of the pair spectrum is complicated by the fact that several inequivalent pair types must be considered. Progress has been made in the interpretation of the optical pair spectrum by measurement of the temperature dependence of the lines[7–9] and by measurement of the stress dependence of the lines.[10]

The simplest theory of the ground-state interaction between two Cr^{3+} ions assumes an interaction of the form $-J\mathbf{s}_1\cdot\mathbf{s}_2$, where $\mathbf{s}_1$ and $\mathbf{s}_2$ are the total electron spins of ions 1 and 2, respectively. For the ground state in ruby, $|\mathbf{s}_1|$ and $|\mathbf{s}_2|$ each have the value $\frac{3}{2}$. The two spins can couple to give a resultant spin of $S=0$, 1, 2, or 3. According to whether J is positive or negative, one has ferromagnetic coupling or antiferromagnetic coupling. The level spacings follow the Lande-interval rule.

From Kisliuk and Krupke[9] and Mollenauer,[10] one kind of Cr^{3+} pair has energy levels at 0, 20.4, 35.0, and 42.9 cm^{-1} (probably fourth-nearest neighbors), while another kind of Cr^{3+} pair has levels at 0, 10.3, 32.7, and 67.9 cm^{-1} (probably second-nearest neighbors). An earlier analysis by Kisliuk, Schawlow, and Sturge[7] gave levels at 0, 33, 99, and 198 cm^{-1} for the second-nearest neighbors, but this was based in part on an optical-absorption line which was found later to be a sharp vibronic feature and not a pair line.[9]

In 1964, Hadni reported the observation of two far i.r. absorption lines in a specimen of concentrated ruby less than 1-cm long.[2] He reported one line at 37 cm^{-1} and a second line at 100 cm^{-1}. These lines were electric-dipole lines and were polarized perpendicular to the optic axis of the crystal. They persisted at helium and hydrogen temperatures, while the 37-cm^{-1} line completely disappeared at nitrogen temperature and the 100-cm^{-1} line nearly disappeared at nitrogen temperature. Each line gave a maximum absorption coefficient on the order of 1 cm^{-1} for a 1.2% concentration of chromium ions. Hadni assigned the two lines to Cr^{3+} pairs. He found a correspondence with the antiferromagnetically coupled second neighbors energy assignment of Kisliuk, Schawlow, and Sturge, which however, is now known to be incorrect.

Transitions between different spin states are forbidden. One might expect this selection rule to be fairly rigidly obeyed for Cr^{3+} pairs in ruby because the ground state of the single Cr^{3+} ion in Al_2O_3 has no orbital angular momentum. Hence, spin-orbit effects (which might relax selection rules) are absent. The lines observed by Hadni seemed surprisingly strong for transition between states of different spins. For the reasons stated above, it was decided to restudy the far infrared absorption of ruby.

B. The Experiment

A very large ruby rod with 1% chromium ion concentration was available for the experiment. The rod was in the form of a right circular cylinder with a 6-in. length and a $\frac{5}{8}$-in. diam. The optic axis of the crystal was at an angle of 60° with respect to the cylinder axis. The sample was mounted at the bottom of the large metal Dewar in a specially designed sample holder. The sample holder was a concentric cylinder that allowed cryogenic liquid (in this case helium) to contact the sample over most of its area. Two indium O-ring seals prevented the liquid helium from leaking through the Dewar compartment and at the same time locked the sample in place. The sample extended approximately $\frac{1}{2}$-in. beyond the O-ring seal on each end. This sample-holding technique ensured that the sample was very close to 4.2°K.

For this experiment, unpolarized far i.r. radiation was transmitted along the length of the ruby cylinder. If the optic axis had been along this direction and if Hadni's interpretation were correct, then there should have been essentially 100% absorption at 37 and 100 cm^{-1} for such a long sample. Taking into account the fact that the optic axis was at 60° with respect to the radiation, there still should have been absorptions (at 37 and 100 cm^{-1}) greater than 60%.

No absorption at all was observed throughout the entire range of the instrument with the exception of the

[4] Y. Tanabe and S. Sugano, J. Phys. Soc. Japan **13**, 880 (1958).
[5] S. Sugano and I. Tsujikawa, J. Phys. Soc. Japan **13**, 899 (1958).
[6] A. L. Schawlow, D. L. Wood, and A. M. Clogston, Phys. Rev. Letters **3**, 271 (1959).
[7] P. Kisliuk, A. L. Schawlow, and M. D. Sturge, in *Advances in Quantum Electronics. Second International Conference in Quantum Electronics, Berkeley, California*, edited by J. R. Singer (Columbia University Press, New York, 1964), p. 725.
[8] P. Kisliuk, Appl. Phys. Letters **3**, 215 (1963).
[9] P. Kisliuk and W. F. Krupke, J. Appl. Phys. **36**, 1025 (1965).
[10] L. F. Mollenauer, Ph.D. dissertation, Stanford University, Stanford, California, 1965 (unpublished).

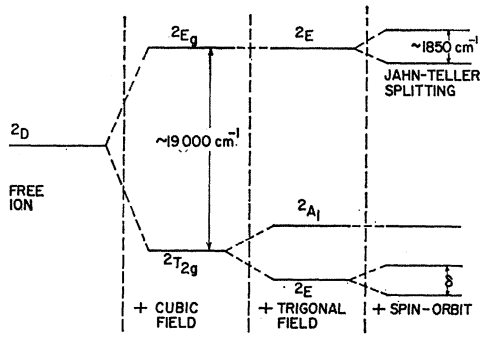

FIG. 2. Energy-level diagram of Al_2O_3:Ti^{3+} with crystalline and spin-orbit interactions.

broad lattice absorption that increased drastically beyond 100 cm^{-1}. An absorption of 10% could have been detected throughout most of the instrument's range. In the region greater than about 125 cm^{-1}, the lattice absorption caused the sensitivity to decrease rapidly. In the region less than about 15 cm^{-1}, the sensitivity decreased (to about 20% at 12 cm^{-1}) because of the inherent loss of sensitivity of the spectrometer at long wavelengths.

This experiment has shown that the 37- and 100-cm^{-1} lines observed by Hadni are not due to Cr^{3+} ion pairs. Furthermore, since it is known that there do exist low-lying pair levels with far-i.r. energy spacings, this experiment also has shown that any transitions between the different spin states must be quite weak—as expected.

The upper limit for oscillator strengths of such pair transitions can be estimated from the results of this experiment with the aid of Eq. (3.1)[11]:

$$k_0=0.025(Nf/\Delta\nu). \qquad (3.1)$$

Equation (3.1) gives the peak absorption coefficient (k_0) for a Gaussian line arising from a sample with N pairs per cm^3 in the lower state and none in the upper state. The oscillator strength is denoted by f and the linewidth (in cps) is denoted by $\Delta\nu$. Assuming a random distribution of Cr^{3+} ions among the aluminum sites in our sample, we estimate $f<(7.2/n)\times10^{-9}$ for σ polarization and $f<(1.2/n)\times10^{-8}$ for π polarization. Here n is the number of equivalent positions for the second ion of a particular pair type. For first- and fifth-nearest neighbors, n equals 1; for second-, third-, and fourth-nearest neighbors, n equals 3.[10]

The apparent explanation of Hadni's result is that he observed lines due to some impurity other than Cr^{3+} pairs. A theoretical study was made to determine what ions in corundum (Al_2O_3) might give absorptions in the far i.r. The Ti^{3+} ion is just such an ion and it is discussed in Sec. IV.

[11] A. L. Schawlow, in *Proceedings of the International School of Physics "Enrico Fermi," Course XXXI, Quantum Electronics and Coherent Light, 1963*, edited by P. A. Miles (Academic Press Inc., New York, 1964).

IV. Al_2O_3:Ti^{3+}

A. Introduction

A consideration of the first transition series of elements showed that the Ti^{3+} ion is one of the most likely to give far i.r. splittings of the ground state when it replaces an Al^{3+} ion in corundum. Figure 2 shows the energy-level scheme for Ti^{3+} in corundum. Since the free-ion configuration consists of a single $3d$ electron outside a closed argon shell, the free-ion level is the 10-fold degenerate ^2D. The crystal field seen by the titanium ion can be divided into a large cubic field and a much smaller trigonal field. Symmetry considerations determine qualitatively how the crystal-field environment splits up the degenerate free-ion level. The cubic field alone splits the 10-fold degenerate ^2D level into a four-fold degenerate ^2E_g and a six-fold degenerate $^2T_{2g}$, with the $^2T_{2g}$ level lower as shown. Addition of the trigonal field does not further split the ^2E_g, but it does split the $^2T_{2g}$ into a doubly degenerate $^2A_1$ and a four-fold degenerate ^2E. Whether the $^2A_1$ or the ^2E is the lower level depends on the sign of the trigonal field. For Ti^{3+} in corundum, the ^2E level actually is the lower level. The reason for this assignment is discussed later. Upon inclusion of the spin-orbit interaction, one finds that the ground-^2E level splits into two doubly degenerate levels. According to McClure,[12] the ^2E excited state is about 19 000 cm^{-1} above the ground state and is split by 1850 cm^{-1} by a Jahn-Teller effect. Thus, the original 10-fold degenerate level of the free ion has been split into five doubly degenerate Kramers levels. These Kramers doublets can be split only by the application of a magnetic field. The splitting of the ground ^2E level by spin-orbit coupling would be expected to be in the far i.r. region.

Two different groups (Kask *et al.*[13] and Feldman *et al.*[14]) have performed spin-resonance experiments on the ground state of Al_2O_3:Ti^{3+}. They both find that $g_{\parallel}\sim1.07$ and $g_{\perp}$ is too small for accurate measurement. The fact that the measured g is so anisotropic indicates that the ground state cannot be the $^2A_1$ level. Since the $^2A_1$ level has no orbital angular momentum, its g value must be isotropic and must have the value ~2.

Both groups have measured the spin-lattice relaxation time T_1 of the ground level as a function of temperature. This T_1 is the time constant for the return to thermal equilibrium of the populations of the 2 sublevels of the ground state after their populations have been disturbed from the equilibrium value by some means. They find that in the temperature region from ~3 to ~14°K (Kask *et al.* measured only to 9°K) T_1

[12] D. S. McClure, J. Chem. Phys. 36, 2757 (1962).

[13] N. E. Kask, L. S. Kornienko, T. S. Mandel'shtam, and A. M. Prokhorov, Fiz. Tverd. Tela 5, 2306 (1963) [English transl.: Soviet Phys.—Solid State 5, 1677 (1964)].

[14] D. W. Feldman, D. C. Burnham, and J. G. Castle, Jr., Westinghouse Research Laboratories, Quarterly Scientific Report No. 4, 1964 (unpublished), Contract No. AF 19(628)1640, AFCRL 64-665.

is given very well by the expression

$$1/T_1 = Ae^{-\delta/kT}. \quad (4.1)$$

This temperature dependence is characteristic of a relaxation process known as the Orbach process.[15] It is a two-step process involving an intermediate level at energy δ above the ground state. The first step is to excite an ion from the excessively populated sublevel of the ground state to the level at energy $\sim\delta$ above the ground state by the absorption of a phonon of energy $\sim\delta$. Then, in a second step, the ion can fall down to the underpopulated sublevel of the ground state with the emission of a phonon of energy $\sim\delta$. Of course, the reverse process will also occur, but the process causing return to thermal equilibrium is favored. From the measured temperature dependence of T_1, Feldman's group estimated δ to be 36 ± 1 cm^{-1}, whereas the Kask group estimated δ to be 30 ± 3 cm^{-1}. Thus, the spin-resonance relaxation measurements indicate that the spin-orbit splitting of the ground state of Ti^{3+} in corundum does indeed fall in the far i.r. The Feldman group further found the value of A in Eq. (4.1) to be 2.5×10^{10} sec^{-1}. This value will be mentioned later, when the lifetime of the level at energy δ above the ground state is discussed.

B. The Far Infrared Absorption Spectrum

It was decided to look for the splitting of energy δ in titanium-doped corundum. Furthermore, although the $^2A_1$ level would normally be expected to be more than 500 cm^{-1} above the ground state,[12] a search for this level up to 162 cm^{-1} (the limit of the instrument) was planned.

Several rock-shop quality corundum samples that would be expected to have titanium as an impurity were obtained and analyzed for impurity content. Two samples containing significant amounts of titanium were run on the far i.r. spectrometer at 4.2°K and showed lines at 37.8 and 107.5 cm^{-1}. A tentative assignment of these absorptions to the energy-level scheme of Fig. 2 was made and two "high-quality" oriented samples of titanium-doped corundum were ordered from Union Carbide, Linde Division.

The common oxide of titanium is rutile (TiO_2) in which the titanium ion is in the +4 oxidation state. This oxidation state corresponds to a closed-shell configuration and is the most stable. For this reason there is a large uncertainty about the amount of Ti^{3+} existing in a titanium-doped corundum sample. Although the total amount of titanium in a sample can be analyzed, there is no way of telling (quantitatively) how much is in the +3 oxidation state. If g values are accurately known, a spin-resonance measurement can determine oxidation states at least semiquantitatively. If one knows the sensitivity of his equipment and the g values of a particular level of a particular oxidation state, then the number of spins corresponding to a given signal strength is known. Unfortunately, as mentioned in Sec. IV.A, g_1 for the ground state of $Al_2O_3:Ti^{3+}$ is very close to zero and very uncertain. Consequently, a "spin-count" determination of the actual amount of Ti^{3+} in a sample is not feasible.

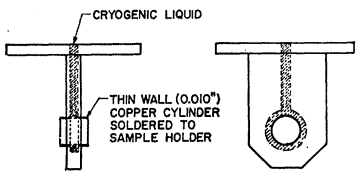

FIG. 3. Sample holder.

Since the +4 oxidation state of titanium is the most stable, there appears to be great difficulty in putting a significant amount of titanium in Al_2O_3 without disturbing the crystal structure. The titanium tends to precipitate out into the rutile structure. Instructions given to Linde indicated that the boule should be grown under reducing conditions so as to enhance the number of +3 ions.

Linde was unable to grow a boule that did not crack at some point in the processing. Whether this situation was caused by the tendency of titanium to form the rutile structure is not known. At any rate, a cracked boule was obtained with $\sim0.15\%$ (by weight of the most common oxide TiO_2) total titanium concentration. The boule was approximately 2-in. long and $\frac{1}{2}$-in. in diam. The boule was intact, but a spiraling crack ran along its length. The optic axis is along the geometric axis of the boule. All the results presented here were obtained with samples cut from this boule.

Since the samples were cracked and also because they were short, the sample-holding technique of Sec. III was impossible. It was desired to have as little temperature difference as possible between the cryogenic liquid in the Dewar and the sample so that the sample temperature could be taken to be the same as the liquid temperature. For this purpose a special sample holder was constructed.

Figure 3 illustrates the sample holder, which attaches to the bottom of the inner Dewar flask with an indium O-ring seal. The cryogenic liquid surrounds the thin wall copper cylinder as shown. A sample was placed inside the copper cylinder and indium metal was stuffed between the sample and the copper cylinder to give good thermal contact and to fix the sample in place. The distance between liquid and sample was at no time greater than 0.1 cm. We estimate that this sample-holding technique ensured that the sample temperatures were always within 0.2°K of the liquid temperature. This difference is negligible for the purposes of this study.

A point of interest resulted from taking preliminary data on the rock-shop samples with the samples immersed in the cryogenic liquid. The far i.r. radiation thus passed through two sapphire windows and the

[15] C. B. P. Finn, R. Orbach, and W. P. Wolf, Proc. Phys. Soc. (London) 77, 261 (1961).

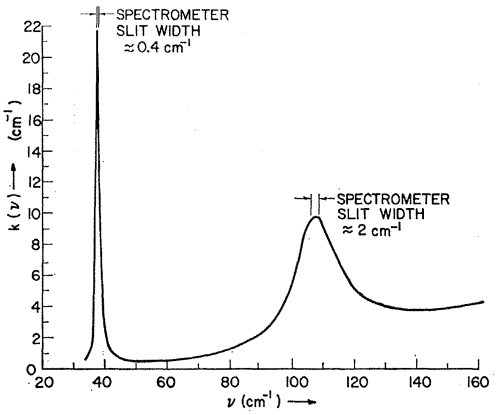

FIG. 4. Axial absorption spectrum of $Al_2O_3:Ti^{3+}$ at 4.2°K. (Total titanium concentration ~0.15%.)

liquid in addition to the sample. Attempts to look at the absorption spectrum of these samples at hydrogen and nitrogen temperatures failed because no far i.r. passed through the sample compartment. It appears that liquid hydrogen and liquid nitrogen absorb far i.r., even though the hydrogen and nitrogen molecules are nonpolar. This situation is an interesting one in itself, but no attempt has been made to investigate it. It is likely that these absorptions arise from dipole moments induced by collisions between molecules of the liquid hydrogen or nitrogen.[16,17] Since the liquid helium molecule is monatomic, no such effect occurs for liquid helium.

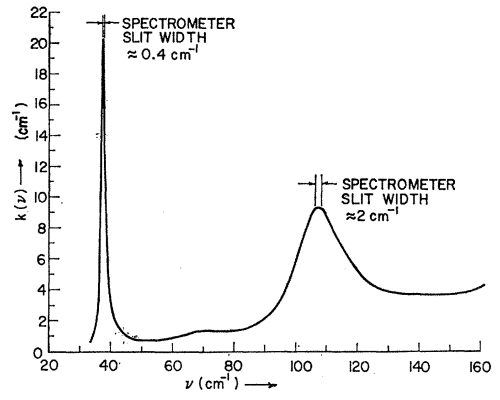

FIG. 5. Axial absorption spectrum of $Al_2O_3:Ti^{3+}$ at 20.3°K.

The absorption spectra were obtained by dividing the signal with a titanium-doped sample in the sample holder by the signal obtained with a pure corundum sample of the same size, shape, and orientation in the sample holder. This proceedure takes into account the absorption of the pure corundum lattice, the reflection losses, and the variation in spectrometer output with wavelength. A small correction should be applied for the effect of multiple reflections, but this correction is less than other uncertainties and so has been neglected. The biggest uncertainty involved in these measurements is the absolute value of the percent transmission. Since the Dewar system has to be disconnected and then reconnected to change from the titanium sample to the pure corundum sample, the accuracy of the absolute percent transmission attributed to Ti^{3+} ions is uncertain by about $\pm 10\%$. This uncertainty will be mentioned again later with regard to line shapes.

Figures 4, 5, and 6 show the results of axial (direction of unpolarized radiation is parallel to the optic axis of the crystal) absorption measurements on the $Al_2O_3:Ti^{3+}$ system at 4.2, 20.3, and 77.4°K, respectively. The

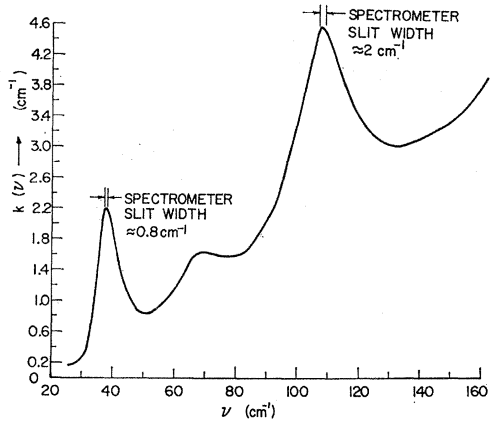

FIG. 6. Axial absorption spectrum of $Al_2O_3:Ti^{3+}$ at 77.4°K.

absorption coefficient $k(\nu)$ is plotted as a function of wave number. It is seen that at all 3 temperatures there is one line at 37.8 cm^{-1} and another at 107.5 cm^{-1}. At 4.2°K, no other lines appear, but at 20.3°K a small absorption appears around 70 cm^{-1}. At 77.4°K, this 70-cm^{-1} absorption becomes more prominent.

The positions and temperature dependence of these lines are consistent with the assumption that they stem from an energy-level diagram such as that shown in Fig. 7. The 70-cm^{-1} line corresponds very closely to the difference between the 37.8- and 107.5-cm^{-1} lines. It appears that the 3 levels shown in Fig. 7 correspond to the 3 lower levels of the Ti^{3+} system—shown in Fig. 2. The value of 37.8 cm^{-1} agrees very well with the values of δ obtained by spin-lattice relaxation measurements of the ground state. As mentioned in Sec. IV.A, the Kask group estimated δ to be 30 ± 3 cm^{-1} and the Feldman group estimated δ to be 36 ± 1 cm^{-1}. The difference be-

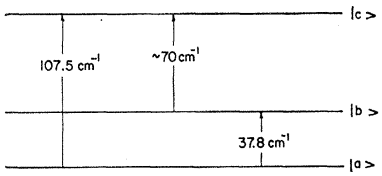

FIG. 7. Observed low-lying energy levels of $Al_2O_3:Ti^{3+}$.

[16] M. F. Crawford, H. L. Welsh, and J. L. Locke, Phys. Rev. 75, 1607 (1949).
[17] D. R. Bosomworth and H. P. Gush, Can. J. Phys. 43, 729 and 751 (1965).

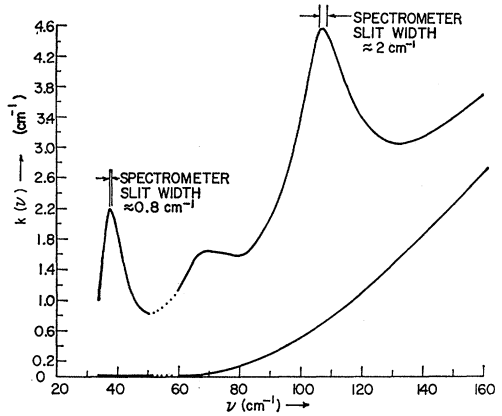

FIG. 8. Polarized absorption spectrum of $Al_2O_3:Ti^{3+}$ at 77.4°K. (Upper curve is for σ polarization. Lower curve is for π polarization.)

tween the directly measured value of δ and those derived from spin-lattice relaxation rates is consistent with the observation by Young and Stapleton[18] that energy gaps predicted by Orbach relaxation rates tend to be less than the directly measured values. They explain this difference in terms of finite level widths.

The maximum absorption coefficient of the 37.8-cm^{-1} line at 4.2 and 20.3°K is quite large (>20 cm^{-1}). For this reason a sample only 1-mm long was used to obtain the data at 4.2 and 20.3°K for this line. At 77.4°K, the maximum $k(\nu)$ for this line is reduced substantially so that a 2-mm sample was used at 77.4°K. [Note that

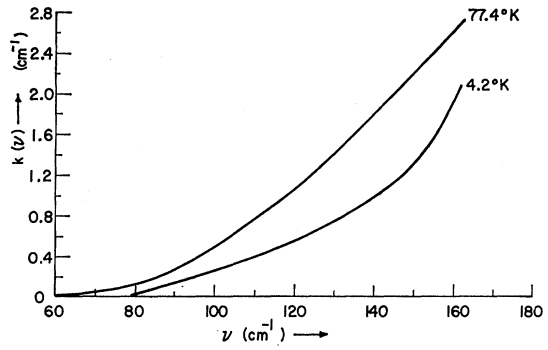

FIG. 9. π absorption spectrum of $Al_2O_3:Ti^{3+}$ at 4.2 and 77°K.

the $k(\nu)$ scale of Fig. 6 is different from those in Figs. 4 and 5.] The 70- and 107.5-cm^{-1} lines were always observed with a 2-mm sample.

An unexpected feature of Figs. 4, 5, and particularly 6 is that the absorption coefficient rises again at wave numbers beyond the 107.5-cm^{-1} line. Unfortunately, $k(\nu)$ is still rising at 162 cm^{-1}, the instrument's limit. This situation was made more clear when polarized spectra were taken.

Figure 8 shows the σ and π spectra at 77.4°K. It is clear that the σ spectrum of Fig. 8 is very nearly the same as the axial spectrum of Fig. 6, while the π spectrum shows none of the 3 lines that appear in the axial spectrum. Consequently, one can conclude that all 3 lines correspond to σ electric-dipole transitions.

The slowly rising characteristic of the π spectrum is suggestive of lattice absorption. The lattice absorption of the pure corundum crystal has already been taken into account. Consequently, the π spectrum is likely to be due to a modification of the lattice absorption by the introduction of titanium. It could be due to Ti^{3+} ions or to a partial modification of the crystal structure by Ti^{4+} ions or some combination of effects. Figure 9 shows the π spectrum at 77.4°K again and compares it to the π spectrum at 4.2°K.

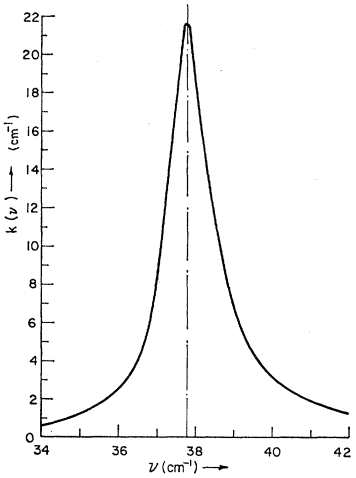

FIG. 10. 37.8-cm^{-1} line of $Al_2O_3:Ti^{3+}$ at 4.2°K.

We have assumed that the slowly varying π spectrum is due to a modification of the lattice absorption and that this π spectrum is unpolarized. Consequently, in order to obtain the true spectrum of the 3 lines, the π spectrum has been subtracted from the axial spectrum.

C. Line Shapes and Linewidths

Figure 10 shows the 37.8-cm^{-1} line at 4.2°K, plotted on an expanded wave number scale compared to that of

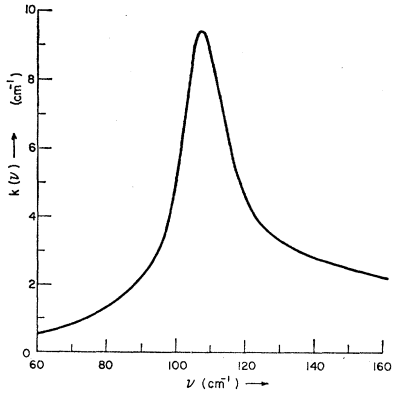

FIG. 11. 107.5-cm^{-1} line at 4.2°K (axial minus π spectrum).

[18] B. A. Young and H. J. Stapleton, Phys. Letters **21**, 498 (1966).

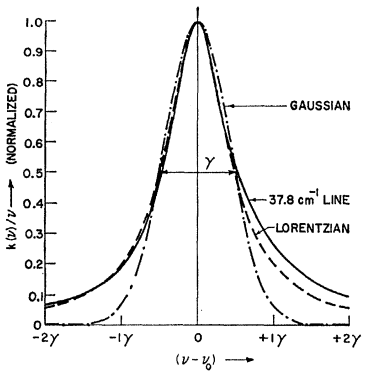

FIG. 12. 37.8-cm^{-1} line shape at 4.2°K, compared with Gaussian and Lorentzian shapes.

Fig. 4 so that the line shape can be seen more easily. Close observation of Fig. 10 shows that the absorption coefficient is not symmetrical about the center frequency. Figure 11 shows the axial minus the π absorption spectrum for the 107.5-cm^{-1} line at 4.2°K. This line shape is clearly not symmetrical about the center frequency. Both lines exhibit the same characteristic of having larger $k(\nu)$ on the high wave number side of the line center than at corresponding points on the low wave number side.

It will be shown that the widths of these lines are predominantly due to lifetime broadening. Ordinarily, a lifetime-broadened line has the familiar symmetrical Lorentzian shape. However, the Lorentzian shape is derived for the condition of very narrow linewidth compared with the center frequency.[19] Since the 37.8- and 107.5-cm^{-1} lines have widths that are not completely negligible with respect to their center frequencies, it is not surprising that they show some asymmetry.

Part of the asymmetry of broad lines can be explained when a distinction is made between the transition-probability shape and the intensity shape ordinarily measured in the laboratory. The transition-probability shape gives the distribution of photons absorbed in an absorption experiment or emitted in a fluorescence experiment. This shape is the normal symmetric Lorentzian if the line is narrow. Since each photon has energy $h\nu$, it follows that the transition-probability shape must be multiplied by ν to give the correct intensity shape. For very narrow lines, ν is very nearly ν_0 (the center frequency) over the entire line. Hence, for narrow lines the transition-probability shape and the intensity shape are the same. However, for a line that has a width that is not negligible compared to ν_0, the shape will become asymmetrical by the ν factor. It should be pointed out that the transition-probability shape itself will deviate from the symmetric Lorentzian when the width is large compared to the center frequency. Messiah shows that this is the case.[19]

If the linewidths observed here are due primarily to lifetime broadening, it is necessary that the line shapes are those appropriate for lifetime broadening. As mentioned above, the Ti^{3+} lines are broad enough so that some deviation from the Lorentzian shape is expected; but they still should show a resemblance to the Lorentzian shape. Figures 12 and 13 show the normalized $k(\nu)/\nu$ at 4.2°K [i.e., $(k(\nu)/\nu)/(k(\nu)/\nu)_{\max}$] versus $(\nu-\nu_0)$ for the 37.8- and 107.5-cm^{-1} lines, respectively. The $k(\nu)$ are divided by ν to change the measured intensity shape to a transition-probability shape as explained above. For comparison purposes, the normalized Lorentzian ($[(\nu-\nu_0)^2+\frac{1}{4}\gamma^2]^{-1}$) and the normalized Gaussian ($\exp[-4((\nu-\nu_0)/\gamma)^2 \ln 2]$) shapes are given also.

For both lines the transition-probability shape clearly fits the Lorentzian shape more closely than the Gaussian. It was stated in Sec. IV.B that there is an uncertainty of $\sim\pm 10\%$ in the absolute value of the percent transmission measured. This uncertainty in percent transmission corresponds to an uncertainty in the base lines of Figs. 10 and 11 of $\sim\pm 0.5$ cm^{-1}. It is clear that this error can affect the shapes in Figs. 12 and 13 that were obtained from Figs. 10 and 11 by dividing the curves by ν. However, this error cannot possibly change the fact that the curves in Figs. 10 and 11 are not symmetrical. Allowance for the uncertainty of the base lines in Figs. 10 and 11 can produce a better fit to the Lorentzian in Figs. 12 and 13, but it is impossible to fit the Gaussian. Therefore, on the basis of line shapes it appears that the measured linewidths are due primarily to lifetime broadening.

In order to obtain linewidths, all the lines were plotted in terms of transition-probability shapes because the linewidths obtained from this kind of curve are the ones related to the lifetimes of the states involved. The measured linewidths for the 37.8-cm^{-1} line at 4.2 and 20.3°K are partially instrument limited; all the other measured linewidths are so large that they are not instrument limited. Section IV.D shows that the temperature dependence of these lines (below 77.4°K) is consistent with direct-process phonon broadening.

D. Linewidth Theory

Since the 37.8- and 107.5-cm^{-1} line shapes at 4.2°K approximate the Lorentzian shape, it is assumed that

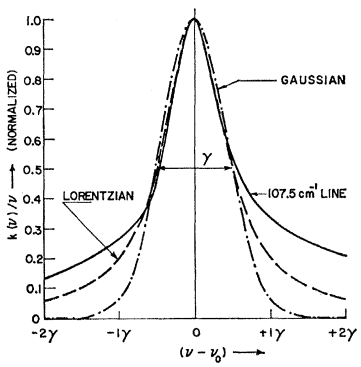

FIG. 13. 107.5-cm^{-1} line shape at 4.2°K, compared with Gaussian and Lorentzian shapes.

[19] A. Messiah, *Quantum Mechanics* (John Wiley & Sons, Inc., New York, 1962), Vol. II, p. 994.

TABLE I. Comparison between calculated and measured linewidths.

	4.2°K		20.3°K				77.4°K			
	γ(cm^{-1}) Measured		γ(cm^{-1}) Measured		γ(cm^{-1}) Calculated		γ(cm^{-1}) Measured		γ(cm^{-1}) Calculated	
ν(cm^{-1})	Min	Max	Min	Max	Min	Max	Min	Max	Min	Max
37.8	~1	~1	$\gtrsim$1	$\gtrsim$1	~1+0.16	~1+0.28	7.2	9.2	5.0	9.2
70.0	...	...	...	...	...	...	25.0	35.0	24.7	36.2
107.5	18.4	20.4	19.2	21.2	19.5	20.8	23.8	28.8	26.5	27.6

the widths are due to lifetime broadening. Because the radiative lifetimes are far too long to give the observed widths, it is further assumed that the lifetimes of the states involved are shortened by interaction with the crystal-lattice vibrations.

The usual ideas of lifetime τ and constant transition probability per unit time $w=1/\tau$ are strictly valid only for the case where linewidths are small compared to center frequency. In this approximation the time dependence of a decaying state is exponential, implying a constant transition probability per unit time. This exponential dependence is usually just assumed, but Messiah shows that it follows from the assumption of narrow lines.[19] The exponential time dependence of a decaying state implies a Lorentzian line shape and vice versa. Although the lines considered here are broad enough to deviate somewhat from the Lorentzian shape, it is assumed that they are narrow enough so that the usual ideas of lifetime and constant transition probability per unit time are valid.

Under consideration here is the 3 level system of Fig. 7. The 37.8-cm^{-1} line corresponds to a transition from $|a\rangle$ to $|b\rangle$, while the 107.5-cm^{-1} line corresponds to a transition from $|a\rangle$ to $|c\rangle$. The 70-cm^{-1} line corresponds to a transition from $|b\rangle$ to $|c\rangle$. At 4.2°K there are very few phonons in a crystal with energy as great as 37.8 cm^{-1}. Consequently, the measured lifetime-determined widths of the 37.8- and 107.5-cm^{-1} lines at 4.2°K must be caused by spontaneous emission of phonons. The 37.8-cm^{-1} line can be broadened by the spontaneous emission of a phonon of energy 37.8 cm^{-1} with the simultaneous relaxation from electronic level $|b\rangle$ to $|a\rangle$. The 107.5-cm^{-1} line can be broadened by the spontaneous emission of a phonon of energy 107.5-cm^{-1} with the simultaneous relaxation from electronic level $|c\rangle$ to $|a\rangle$, or it can be broadened by the spontaneous emission of a phonon of energy 70 cm^{-1} with simultaneous relaxation from electronic level $|c\rangle$ to $|b\rangle$. As the temperature is raised, more phonons will exist with higher energies and the processes mentioned above will be enhanced by absorption and stimulated emission of phonons.

It is assumed at first that only such direct phonon processes are important up to 77.4°K. A direct process is one that connects two electronic levels with a single phonon created or destroyed to conserve energy. Higher-order processes, such as the two-phonon Raman process, will become important at higher temperatures. When the linewidths become larger than those predicted by direct processes, then the higher-order processes may be assumed to become important.

Let the linewidths of the 37.8-, 107.5-, and 70-cm^{-1} lines be denoted by γ_{ab}, γ_{ac}, and γ_{bc}, respectively. Also, let $\Delta_{ab}=37.8$ cm^{-1}, $\Delta_{ac}=107.5$ cm^{-1}, and $\Delta_{bc}=70$ cm^{-1}. Then, considering only direct-process phonon relaxation among the levels $|a\rangle$, $|b\rangle$, and $|c\rangle$ of Fig. 7, we obtain

$$\gamma_{ab}=K_{ab}\left(\frac{2}{(e^{\Delta_{ab}/kT}-1)}+1\right)+K_{ac}\left(\frac{1}{(e^{\Delta_{ab}/kT}-1)}\right)+K_{bc}\left(\frac{1}{(e^{\Delta_{bc}/kT}-1)}\right), \quad (4.2)$$

$$\gamma_{ac}=K_{ab}\left(\frac{1}{(e^{\Delta_{ab}/kT}-1)}\right)+K_{ac}\left(\frac{2}{(e^{\Delta_{ac}/kT}-1)}+1\right)+K_{bc}\left(\frac{1}{(e^{\Delta_{bc}/kT}-1)}+1\right), \quad (4.3)$$

and

$$\gamma_{bc}=K_{ab}\left(\frac{1}{(e^{\Delta_{ab}/kT}-1)}+1\right)+K_{ac}\left(\frac{1}{(e^{\Delta_{ac}/kT}-1)}+1\right)+K_{bc}\left(\frac{2}{(e^{\Delta_{bc}/kT}-1)}+1\right), \quad (4.4)$$

where K_{ab}, K_{ac}, and K_{bc} are independent of temperature.

At 4.2°K, Eq. (4.2) gives $\gamma_{ab}(4.2°\text{K})=K_{ab}$, and Eq. (4.3) gives $\gamma_{ac}(4.2°\text{K})=K_{ac}+K_{bc}$. But $\gamma_{ab}(4.2°\text{K})$ has been measured to be ~1 cm^{-1}, so $K_{ab}\sim1$ cm^{-1}. Also, $\gamma_{ac}(4.2°\text{K})$ has been measured to be 19.4±1 cm^{-1}, so $K_{ac}+K_{bc}=19.4\pm1$ cm^{-1}. Equation (4.4) gives $\gamma_{bc}(77.4°\text{K})=1.98K_{ab}+1.16K_{ac}+1.75K_{bc}$. Using $K_{ab}\sim1$ cm^{-1}, we get $\gamma_{bc}(77.4°\text{K})=2.18+1.16K_{ac}+1.75K_{bc}$. Since the coefficient of K_{ac} is less than that of K_{bc}, and since $K_{ac}+K_{bc}\sim19.4$ cm^{-1}, the maximum calculated value for $\gamma_{bc}(77.4°\text{K})$ will be obtained if $K_{ac}=0$ and $K_{bc}=19.4$ cm^{-1}. The minimum calculated value for $\gamma_{bc}(77.4°\text{K})$ will be obtained if $K_{ac}=19.4$ cm^{-1} and $K_{bc}=0$. The values so calculated are $\gamma_{bc}(77.4°\text{K})=36.2$ cm^{-1} (max), 24.7 cm^{-1} (min). Since these values correspond to about the same range of uncertainty as estimated from our data, the maximum and minimum values of the other lines are calculated here by taking $K_{ac}=0$, 19.4 cm^{-1} and $K_{bc}=19.4$ cm^{-1}, 0. The large

uncertainty in the measured value of $\gamma_{bc}(77.4°K)$ is due to the fact that the 3 lines are overlapping. Since the coefficient of K_{ac} is less than that of K_{bc} in the expression for each linewidth at each temperature measured, the calculated linewidths are all maximum or all minimum at the same time.

Table I shows the results of calculation of the linewidths from Eqs. (4.2), (4.3), and (4.4), together with the measured values for comparison. It is seen that the calculated values are consistent with the measured values. Consequently, it appears that the linewidths of this system at temperatures below 77.4°K are determined primarily by direct-process phonon broadening.

E. Discussion of Results

The chief results of this study of $Al_2O_3:Ti^{3+}$ are: (1) The previously undetermined low-lying energy-level diagram has been determined. (Although spin resonance had predicted the approximate position of the 37.8-cm^{-1} line, the direct measurement is more accurate. The 107.5-cm^{-1} level not only was unknown previously, but it has a surprisingly low value. This result will be discussed somewhat later.) (2) The linewidths of this system have been measured and explained. On the basis of these linewidths and the line shapes it has been shown that the lifetimes of the levels involved are severely limited by direct-process phonons. (A 1-cm^{-1} linewidth corresponds to a lifetime $\tau=1/2\pi c\gamma=5.3\times10^{-12}$ sec. Even at absolute zero temperature the lifetimes will be severely limited by spontaneous emission of phonons.)

The positions of the first two energy levels above the ground state for $Al_2O_3:Ti^{3+}$ do not agree well with crystal-field theory. These two levels would normally be expected to be at $\sim\frac{3}{4}\xi$ and $\sim v+\frac{3}{4}\xi$ above the ground state, where ξ is the spin-orbit parameter (normally $\xi\sim100$ cm^{-1}) and v is the trigonal parameter.[20] The Kask[13] and Feldman[14] spin-resonance groups mentioned earlier both suggested that the spin-orbit splitting might be reduced by covalency. McClure[12] has studied the optical spectra of Ti^{3+}, V^{3+}, Cr^{3+}, Mn^{3+}, Co^{3+}, and Ni^{3+} in corundum and found values of the trigonal field-splitting parameter v for all ions but Ti^{3+}. For all the other ions, v is between 720 and 1950 cm^{-1}, whereas the results presented here indicate that v for Ti^{3+} is less than the values for the other ions by perhaps an order of magnitude. It is possible that a dynamical Jahn-Teller effect is at work here to reduce the trigonal and spin-orbit parameters.[21] At any rate, something more than ordinary crystal-field theory is necessary to explain the $Al_2O_3:Ti^{3+}$ system.

Although McClure did not find a value for the trigonal splitting parameter v from his optical data, he did indicate that v should be greater than 500 cm^{-1}. He made this estimate from the temperature dependence of the polarization character of the absorption band centered at $\sim$19 000 cm^{-1}. This band corresponds to absorption from the components of the $^2T_2$ level to the excited ^2E level (see Fig. 2). He determined the integrated absorption coefficient over the band for both π and σ polarizations and found that the ratio of π to σ integrated absorption coefficients remained nearly constant at 3.2 from 77°K all the way up to 800°K. Since absorption from the $^2A_1$ component of the $^2T_2$ state to the excited ^2E state is forbidden in π polarization (but not in σ) by trigonal selection rules, he expected the ratio of π to σ to decrease when the temperature was high enough to populate the $^2A_1$ level. Since he observed no such effect up to 800°K, he concluded that v must be greater than 500 cm^{-1}. However, it has been shown here by the direct far i.r. measurement that the $^2A_1$ level lies only 107.5 cm^{-1} above the ground state. This value implies that $v\sim100$ cm^{-1}. To reconcile this result with that of McClure, it is proposed that either: (1) although the absorption from the $^2A_1$ level is allowed in σ polarization, its strength is much less than that of the absorption from the ^2E component of the $^2T_2$ level; or (2) the selection rules for pure electronic transitions differ from the rules for the vibronic transitions giving rise to the band.

The selection rules for the 37.8- and 107.5-cm^{-1} lines predict σ polarization for both lines, in agreement with what has been measured. The selection rules for the 70-cm^{-1} line will allow both σ and π. Since only σ has been measured, the intensity of the π transition must be much weaker than that of the σ.

For direct phonon relaxation from the Kramers doublet $|b\rangle$ to the Kramers doublet $|a\rangle$ in Fig. 7, two transition rates (W_1 and W_2) are sufficient to describe the relaxation. Since $|b\rangle$ and $|a\rangle$ each have two states, there are four possible transitions between $|b\rangle$ and $|a\rangle$. However, it can be shown that, for Kramers doublets, the two spin-flip transitions have equal transition rates and the two no spin-flip transitions have equal transition rates.[22] Call the spin-flip transition rate W_1 and call the no spin-flip rate W_2. According to Yen *et al.*,[23] the Orbach coefficient A in Eq. (4.1) is given in terms of W_1 and W_2 by

$$A=4W_1W_2/(W_1+W_2). \tag{4.5}$$

The total transition rate *out* of $|b\rangle$ (at 4.2°K) is just W_1+W_2. Thus, the width of level $|b\rangle$ (at 4.2°K) is given by

$$\gamma_b(4.2°K)=(W_1+W_2)/2\pi c. \tag{4.6}$$

The measured linewidth of the 37.8-cm^{-1} line at 4.2°K ($\sim$1 cm^{-1}) is just $\gamma_b(4.2°K)$. Putting $\gamma_b=1$ cm^{-1} in (4.6) gives $W_1+W_2=18.8\times10^{10}$ sec^{-1}. Feldman, Burnham, and Castle[14] have found the A in (4.5) to have the value 2.5×10^{10} sec^{-1}. Putting in these values for

[20] R. M. Macfarlane (private communication).
[21] F. S. Ham, Phys. Rev. **138**, A1727 (1965).
[22] P. L. Scott, Ph.D. dissertation, University of California, Berkeley, California, 1960 (unpublished).
[23] W. M. Yen, W. C. Scott, and P. L. Scott, Phys. Rev. **137**, A1109 (1965).

W_1+W_2 and for A into (4.5), one obtains $W_1=0.65\times10^{10}$ sec^{-1} and $W_2=18.15\times10^{10}$ sec^{-1}. Thus, the no spin-flip transition rate is about 28 times the spin-flip transition rate. (Actually it has been *assumed* that the spin-flip rate is slower than the no spin-flip rate; it is reasonable to assume that the electric field of the lattice vibrations is more likely to induce no spin-flip transitions than spin-flip transitions.) This difference in rates is quite reasonable. For example, Blume *et al.*,[24] have calculated the spin-flip transition from the $2\bar{A}$ level to the $\bar{E}$ level in ruby to be $\sim$60 times slower than the corresponding no spin-flip transition.

V. CONCLUSIONS

We have shown that far i.r. lines previously attributed to Cr^{3+} pairs in concentrated ruby must be due to some other impurity and not to Cr^{3+} pairs. Furthermore, we have shown that transitions between different spin states of an exchange coupled pair of Cr^{3+} ions in Al_2O_3 must be quite weak. This result indicates that such transitions between different spin states of exchange-coupled pairs, in general, should be quite weak when spin-orbit coupling is unimportant.

It has been shown that the lifetimes of the low-lying levels of the $Al_2O_3:Ti^{3+}$ system are extremely short because of the interaction with phonons of the same energy as the far i.r. level spacings. To the authors' knowledge, this study is the first to specifically determine the level widths and, hence, the lifetimes of far i.r. levels of ions in crystals. The lifetimes of far i.r. levels of ions in crystals normally would be expected to be drastically shortened by phonons with far i.r. energies, but more work needs to be done to determine the strength of the phonon interaction with other ions in other crystals. A few general remarks as to the possibility of finding far i.r. levels of ions in crystals that have little interaction with the phonons of the crystal are made here. A similar discussion has been given by Varsanyi.[25]

An interesting comparison can be made between the low-temperature lifetime of the level $|b\rangle$ of the 37.8-cm^{-1} line of $Al_2O_3:Ti^{3+}$ and the low-temperature lifetime of the $2\bar{A}$ level in ruby (as calculated by Blume *et al.*[24]). In the Ti^{3+} case, the lifetime is determined by the spontaneous emission of phonons of energy 37.8 cm^{-1} with the simultaneous relaxation from $|b\rangle$ to $|a\rangle$. In the ruby case, the lifetime is determined by the spontaneous emission of phonons of energy 29 cm^{-1} with the simultaneous relaxation from the $2\bar{A}$ level to the $\bar{E}$ level. The low-temperature lifetime of the $|b\rangle$ level in $Al_2O_3:Ti^{3+}$ has been shown here to be $\sim5\times10^{-12}$ sec, whereas Blume *et al.* calculate the low-temperature lifetime of the $2\bar{A}$ level in ruby to be $\sim3\times10^{-10}$ sec. Thus, the $|b\rangle$ level of $Al_2O_3:Ti^{3+}$ has a low-temperature lifetime about 60 times shorter than the corresponding lifetime for the $2\bar{A}$ level of ruby. In order to calculate any coupling at all (via phonons) between the $2\bar{A}$ and $\bar{E}$ levels in ruby, Blume *et al.* were forced to admix some of the higher $^2T_2$ (cubic) level into the $2\bar{A}$ and $\bar{E}$ levels. On the other hand, the $|b\rangle$ and $|a\rangle$ levels of $Al_2O_3:Ti^{3+}$ can be connected by phonons (as far as selection rules are concerned) without the admixing of higher levels. Thus, it seems reasonable that the Ti^{3+} system $|b\rangle$ level has a shorter low-temperature lifetime than the $2\bar{A}$ level of ruby.

There are two circumstances under which the effect of direct-process phonons on the lifetimes of electronic levels of ion in crystals could be small. First is the circumstance in which there are few phonons available with the correct energy to connect two electronic levels. Second is the case in which the phonons of the correct energy do not strongly couple the electronic levels. Hence, if the maximum phonon energy in a crystal is less than the spacing of the electronic levels under consideration, then there will be no one-phonon (direct) processes connecting these levels. Processes involving two or more phonons must then be considered, but these will in general be weaker. However, even if there are many phonons in a crystal of the correct energy to connect electronic levels, selection rules may prevent such a coupling. It thus appears that a consideration of symmetry is important in the determination of candidates for ions in crystals with long-lived far i.r. levels. Since strong selection rules often arise from highly symmetrical situations, it would appear that cubic crystals, in general, would be the most likely to give little phonon interaction with far i.r. levels of ions.

Because of the fact that phonons do not directly perturb electron spins,[26] there exists the possibility that (with weak spin-orbit coupling) selection rules could forbid phonon relaxation between far i.r. levels while magnetic dipole electronic transitions could still be allowed. In a cubic crystal, with inversion-site symmetry, electric-dipole transitions are forbidden, but magnetic dipole (T_{1g}) electronic transitions may be allowed. Since there are no T_{1g} vibrations of an octahedron, no T_{1g} phonon modes would be available to connect two far i.r. levels. The only octahedral vibrations that can connect two electronic levels of the type considered here are the E_g and T_{2g} vibrations.[26] These E_g and T_{2g} vibrations, however, cannot connect the different spin components of an A_1 level or an A_2 level. Consequently, magnetic dipole electronic transitions between spin components of an A_1 or A_2 (cubic) level may be allowed while phonon relaxation between these components is forbidden. These components may be separated (at far i.r. spacings) by exchange fields in magnetic materials.

[24] M. Blume, R. Orbach, A. Kiel, and S. Geschwind, Phys. Rev. **139**, A314 (1965).

[25] F. Varsanyi, in *Physics of Quantum Electronics*, edited by P. L. Kelley, B. Lax, and P. E. Tannenwald (McGraw-Hill Book Company, Inc., New York, 1966).

[26] J. H. Van Vleck, Phys. Rev. **57**, 426 (1940).

Because phonons interact with electronic states via electric fields,[26] there can be no first-order direct phonon relaxation between the components of a Kramers doublet. If such Kramers doublets could be split with far i.r. separations (either by external magnetic fields or internal exchange fields) then magnetic dipole electronic transitions would be allowed but phonon transitions could be weak.

Impurity-doped crystals have proven to be good laser materials for wavelengths longer and shorter than far i.r. wavelengths. It is possible that doped crystals can be found to serve as laser materials for far i.r. wavelengths also. The investigation of such possibilities as indicated above and other special situations should give interesting results.

ACKNOWLEDGMENTS

We are grateful to Dr. R. M. Macfarlane and Professor P. L. Scott for a number of helpful discussions.

PHYSICAL REVIEW VOLUME 156, NUMBER 2 10 APRIL 1967

Mode Interaction in a Zeeman Laser*

W. CULSHAW AND J. KANNELAUD
Lockheed Palo Alto Research Laboratory, Palo Alto, California
(Received 2 November 1966)

The interaction between modes of a short He-Xe laser using the $J=1 \rightarrow 0$ transition at 2.65 μ is investigated in an axial magnetic field. In zero field an elliptically polarized output usually predominates, with orientation and eccentricity changing with conditions and reflector characteristics. Neutral coupling occurs here; consequently, the system is sensitive to perturbations, in agreement with the observed erratic behavior. Small axial magnetic fields produce circular polarizations, quenching, and hysteresis effects between the two Zeeman oscillations arising from the frequency splitting of a single axial mode. A strong interaction, including sharp crossover regions in the intensities and quenching phenomena, is observed between two axial modes oscillating on well-resolved oppositely circularly polarized Zeeman components. The phenomena are studied as a function of cavity tuning, laser intensity, pressure, and magnetic field. No hysteresis was observed in the interaction between axial modes. The axial-mode intensities are equal for all positions of cavity tuning when the Zeeman separation equals the axial-mode interval. For small deviations of magnetic field from this value, however, crossover and quenching effects appear, and this allows a precise determination of the g value of the upper state. These effects are discussed on the basis of Lamb's theory and equations deduced for the interaction. The Doppler parameter Ku is about 100 Mc/sec for xenon, which is comparable with the natural linewidths, and requires a more exact discussion of the third-order atomic polarization terms. The results derived show some qualitative agreement with observations, particularly on the axial-mode interaction, which is discussed in detail.

I. INTRODUCTION

IN this paper we shall be concerned with the effects of axial magnetic fields on a short He-Xe laser operating on a $J=1 \rightarrow 0$ transition at 2.65 μ. Previous work[1] on the He-Ne, $J=1 \rightarrow 2$ laser transition at 1.153 μ has shown that the polarization of an internal-mirror, or planar-type, laser is linear in zero magnetic field. Also, in near-zero axial magnetic fields, a rotation of this linear polarization occurs up to a maximum of $\pm\frac{1}{4}\pi$, and is a result of a mutual locking of the circularly polarized oscillations due to the proximity of their frequencies. With increasing magnetic field, both circularly polarized oscillations occur simultaneously, and low-frequency beats appear as a result of the frequency splitting of the single axial mode involved.

The results obtained with an axial magnetic field on the He-Xe laser are entirely different in most respects. The occurrence of low-frequency beats seems to be much less pronounced and has not been observed so far. In zero magnetic field, the polarization tends to be circular or elliptical, and only in rare instances in a linear polarization observed at low intensities. Rotations of the elliptic polarization with cavity tuning and magnetic field have been observed at times, but such results are erratic and not reproducible. They are highly dependent on the past history of the system, such as reflector changes, intensity of oscillation and direction of cavity tuning, and on the gas pressure.

The results obtained on the He-Ne transition in near-zero magnetic fields substantiate the result deduced by Heer and Graft[2] that in a $J=1 \rightarrow 2$ transition the singular point representing simultaneous oscillations on both circular polarizations is stable. This result is derived for the laser tuned to the line center, and for perfectly isotropic reflectors. The presence of a small anisotropy in the reflectors, and the near coinci-

* Supported by the Lockheed Independent Research Funds.
[1] W. Culshaw and J. Kannelaud, Phys. Rev. **136**, A1209 (1964); **141**, 228 (1966); **141**, 237 (1966).

[2] C. V. Heer and R. D. Graft, Phys. Rev. **140**, A1088 (1965).